

Study of the Gas-Phase Chemistry of RDX: Experiments and Modeling

Thomas A. Litzinger,* Barry L. Fetherolf,† YoungJoo Lee,‡ and Ching-Jen Tang‡
Pennsylvania State University, University Park, Pennsylvania 16802

The objectives of this work were to identify the species produced during the CO₂ laser-induced decomposition of 1,3,5-trinitrohexahydro-s-triazine (RDX) and to obtain species profiles in the gas-phase during laser-assisted combustion for comparison to a one-dimensional model of the flame. In the experiments, a microprobe/mass spectrometer system was used to measure quantitative gas-phase species profiles and a high-magnification video system was used to observe surface behavior and flame structure. Gas-phase species evolved from the surface and also inside a bubble were measured. The species identified at the surface were HCN, NO₂, H₂O, NO, CO, N₂O, N₂, and H₂; no CO₂ was found at the surface. Formaldehyde may have been present, but it could not be unambiguously identified. Species mole fractions measured at 1.0 atm and a heat flux of 400 W/cm² were used as input to a one-dimensional model along with a temperature profile obtained from the literature for similar experimental conditions. In order to obtain reasonable agreement between the model and the experiments for stable species, RDX vapor had to be added to the initial species for the model calculations. However, even with this addition, the profiles for OH and NH did not match data available in the literature.

Introduction

RDX (1,3,5-trinitrohexahydro-s-triazine) is a highly energetic material that is used in solid propellants in artillery guns and rocket motors. It has been the subject of numerous studies, most of which focus on its decomposition into gas-phase species. This literature was reviewed by Boggs¹ and Schroeder² in the mid-1980s, and significant work has been performed since then.^{3–7}

While a substantial amount of work has been performed on RDX decomposition, very few experimental results are available in which gas-phase species profiles above the surface of a deflagrating RDX propellant were measured. The only work that has produced profiles of most of the major stable species is that of Korobeinichev et al.,^{8,9} who performed studies at 0.5, 1, and 2 atm, although only the results at 0.5 atm pressure were published as quantitative data. Recently, Parr and Hanson-Parr¹⁰ have produced quantitative species profiles of NO, NO₂, OH, CN, and NH for RDX during laser-assisted combustion of RDX, using absorption spectroscopy and planar laser-induced fluorescence (PLIF). They also measured the temperature profile in the condensed phase and gas-phase by combining thermocouple, absorption, and PLIF data. In addition, they developed an absorption technique for formaldehyde and applied it to the RDX flame; the maximum mole fraction detected was 0.005 near the sample surface.

In the present work, the decomposition species at low pressures and low heat fluxes during laser-induced decomposition were measured and compared to the decomposition results of other researchers. For conditions similar to those of Parr and Hanson-Parr,¹⁰ the composition of stable species as a function height above the surface were measured to provide a more complete data set for model validation. Finally, the species mole fractions at the sample surface from the present work and the measured temperature profile of Parr and Hanson-Parr were used to model the gas-phase processes using

the kinetics model of Yetter and Dryer¹¹ and the CHEMKIN II code.^{12–15}

Experimental Approach

A schematic diagram of the experimental setup is given in Fig. 1. The energy source of ignition was a high-power CO₂ laser with a maximum continuous wave power of 700 W. The laser beam passed through a mask and an expanding lens before entering the test chamber through a KCl window. The size of the beam was selected to be about twice that of the sample so that a nearly uniform beam profile could be applied to the surface. The RDX samples were 0.64-cm-diam pellets pressed from RDX powder.

The propellant samples were glued to a small block angled at 45 deg to the incident laser beam so that the sampling microprobe approached the sample perpendicular to the center of the sample surface. During a test, the sample was pushed toward the sampling probe by a linear positioner to obtain species profiles. A high-quality Plexiglas® window was installed on one side of the chamber for video photography of the flame and the RDX pellet. The video was acquired using a charged-coupled device (CCD) video camera with a micro-lens; after each test it was used to identify the sampling height, i.e., the distance between the RDX surface and the sampling probe tip. Typically, a magnification of 30–40 times was used

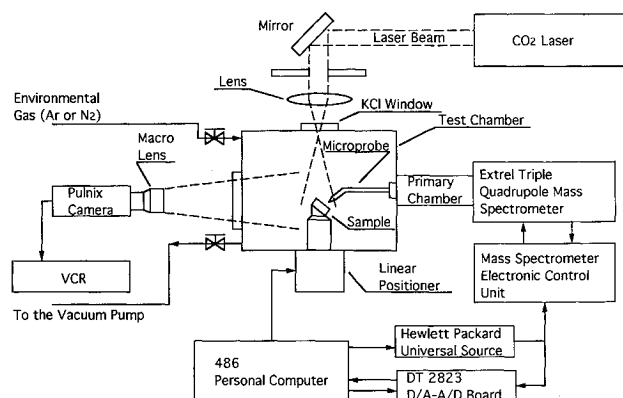


Fig. 1 Experimental setup for microprobe mass spectrometer studies.

Received Aug. 6, 1994; revision received Dec. 9, 1994; accepted for publication Dec. 22, 1994. Copyright © 1995 by the American Institute of Aeronautics and Astronautics, Inc. All rights reserved.

*Associate Professor, Mechanical Engineering.

†Graduate Research Assistant; currently at Martin Marietta Defense Systems, Pittsfield, MA.

‡Graduate Research Assistant.

that produced a spatial resolution of about 20 μm for the videos.

The analysis of gaseous species was performed using a microprobe/mass spectrometer (MPMS) system. The species were sampled by quartz microprobes with an orifice diameter of 20–30 μm , which produced a spatial resolution of 100–150 μm . The sample gases were drawn through the probe and into the mass spectrometer by a set of turbomolecular pumps and vacuum pumps and ionized at the ionizer in the mass spectrometer. In early experiments, to determine the decomposition species, a single quadrupole mass spectrometer was used. In later tests for species profiles the mass spectrometer unit was upgraded to a triple quadrupole mass spectrometer (TQMS) from Extrel. The TQMS was required for these tests to overcome difficulties in differentiating species with the same mass using the single quadrupole mass spectrometer. Differentiating multiple species with the same mass is very difficult with a single quadrupole and requires multiple runs at different ionization energies or the application of a matrix approach to obtaining quantitative data. Using the so-called "daughters" mode of operation of the TQMS, it was possible to identify and differentiate N_2 , CO , C_2H_4 at 28 amu, NO , CH_2O at 30 amu, and N_2O , CO_2 at 44 amu, as well as possible species at 29 amu.

In the daughter mode of operation, the mass of interest, often referred to as the "parent," is selected in the first quadrupole. The parent ions then enter the second quadrupole (Q2) and are fragmented into smaller species, the daughters, by the process of collision-induced dissociation (CID) with an inert gas separately supplied into Q2. Argon was used as the collision gas in this study to minimize its contribution to fragmented masses. The daughters, at masses less than their parent, are detected in the third quadrupole. For complex parent ions, some of the daughters might overlap if the parents contain common structures. In the present study, however, at least one unique daughter could be acquired for each parent. Details of the application of the TQMS to RDX can be found elsewhere.¹⁶

Several methods of calibration were used to obtain the sensitivity coefficients (intensity/concentration) of each species. The most stable species were calibrated directly with the gas mixtures of known concentration. To calibrate water, water vapor was acquired from liquid water that was vaporized by the CO_2 laser. Paraformaldehyde and trioxane, polymeric forms of CH_2O , were used for its calibration. They were also vaporized with the CO_2 laser to obtain gas-phase formaldehyde. Typically, the sensitivity factors were repeatable within 10%. The calibration of species for which standards were not readily available, e.g., HCN , were estimated by correlating the signal intensity to that of calibrated species with a similar appearance potential through the ratio of their cross sections.¹⁷

For all of the calibrations and in the actual tests, an ionization energy of 22 eV was used to minimize fragmentation of molecules and to get acceptable intensities. However, this setting was still high compared to the ionization energies of 9–15 eV for most organic compounds, thus, some fragments were formed and contributed to the signals at masses other than the parent mass. In such instances, these signals were subtracted from the mass signal of interest.

In reducing the experimental data the measured concentrations were totaled and each concentration was divided by the total to get the mole fractions of the sampled gases. This method of calculating normalized mole fractions eliminates the effect of sample temperature on the observed signal intensities since the temperature dependence cancels out. This calculation method also cancels out the effect on signal intensity of probe orifice blockage during a test. The measured mole fractions were then used to perform element balances through the reaction zones as a check on the quality of the data.

In the present set of experiments, measurements of species were obtained at 0.1–1 atm pressure of argon and heat fluxes

of 25–400 W/cm^2 . Low pressure and low heat flux experiments were used in the decomposition studies. For species profiles during laser-assisted combustion at atmospheric pressure, the high heat flux was used to expand the reaction zones and decrease the spatial gradients of various species.¹⁶

Kinetic Modeling

The objective of the kinetic modeling was to validate the detailed model of the gas-phase chemistry for RDX that is being developed by Yetter and Dryer.¹¹ The model was used to generate gaseous species profiles as a function of the height above the material surface that could be compared directly to the experimentally determined species profiles. The gas-phase was modeled as a one-dimensional, laminar, steady flow of a premixed gas mixture at constant pressure. The model was solved with the CHEMKIN II software package^{12–14} and the PREMIX subroutine.¹⁵ Melius¹⁸ has used the same general approach of assuming a premixed flame for his model of RDX combustion and also used the CHEMKIN software to solve the model. Melius considered the condensed phase in the model by treating it as a "pseudogas" with the physical properties of the solid and by adding a single-step condensed-phase decomposition mechanism. Ermolin et al.¹⁹ have also used the one-dimensional, premixed flame approach to model RDX combustion, but modeled only the gas-phase by using the gas composition right at the gas–solid interface, which was measured experimentally,^{8,9} as part of the initial conditions. The latter approach was used in the modeling work presented in this article.

In the current study, the energy equation was not solved, and so the PREMIX subroutine required as input the mass flux from the surface and the temperature profile. The mass flux was calculated by a mass flux balance at the surface using burning rates determined by analysis of the video recordings for each experiment. The experimental temperature profile of Parr and Hanson-Parr¹⁰ was used. Use of this profile should remove much of the uncertainty associated with the presence of the incident heat flux because its effects should be included in the measured temperatures. The remaining input was the final composition expected; this was obtained by determining the equilibrium composition of the input species for the final temperature in the measured temperature profile of Parr and Hanson-Parr.

The kinetic mechanism of Yetter and Dryer¹¹ was employed as the elementary reaction scheme for the model. Their mechanism includes decomposition reactions for the parent RDX molecule and reactions for the larger RDX fragments such as methylene nitramine. The mechanism used for the modeling efforts consisted of 38 species and 178 reactions.

Results and Discussion

The experimental results will be presented and discussed in two different sections, each section representing a distinctly different category of laser-induced behavior. In the first category, denoted "laser-induced decomposition," the sample simply melted and decomposed; it did not exhibit any quasi-steady regression. In the second category of tests, "laser-assisted combustion," the sample regressed in a stable manner with a luminous flame observed above the surface. The results for kinetic modeling of RDX laser-assisted combustion will be presented in a third section.

The results that will be presented here are graphs of species profiles as a function of time for laser-induced decomposition conditions and as a function of the height above the surface for laser-assisted combustion conditions. For the species profile measurements, element conservation was checked as a function of the sampling height, assuming negligible effects of species diffusion.

Laser-Induced Decomposition

Laser-induced decomposition of RDX was observed for tests at pressures of 0.1 or 0.5 atm of argon with an incident

heat flux of 25 W/cm². This work was performed using a single quadrupole mass spectrometer, prior to the acquisition of the triple quadrupole; therefore, identification of species structures was not possible. The first distinct and continuous sign of the onset of pyrolysis was the appearance of a glossy liquid layer on the surface followed by motion of the layer. The motion was seen as both a slight upward expansion of the surface and random boiling motion. The expansion was due to a slight change in density as the material melted and may also be due in part to the evolution of subsurface gases by decomposition of the RDX. Behrens and Bulusu^{3,4} stated that they observed significant quantities of gaseous decomposition products as soon as RDX started to liquefy at 198°C.

Figure 2 displays temporal species profiles for gas sampling about 2.0 mm above an RDX sample surface with an incident heat flux of 25 W/cm² and a pressure of 0.5 atm. In this test, the mass spectrometer was scanning from 15 to 100 amu, and laser heating was terminated at 3 s. Figure 2 displays profiles for the calibrated species in absolute mole percent, i.e., without normalizing the concentrations to obtain mole fractions. The 29-amu signal was converted to a mole fraction using the calibration results for formaldehyde to obtain an approximate value. At 28 amu, the contributions of CO and N₂ could not be separated, and so an average sensitivity factor was used. Finally, the 44-amu signal was converted assuming that no CO₂ existed at the surface of the sample, an assumption that was later verified by TQMS studies.

The video images for the test displayed in Fig. 2 showed that the surface liquid layer boiled vigorously with no luminous emission. The boiling phenomenon lessened after the laser heating was terminated, but still continued to some extent for several more seconds. Liquid material and bubbles growing from the surface layer reached a height of roughly 1 mm during laser heating. However, after laser heating was terminated, a very large bubble formed at the surface and expanded to encompass several millimeters of the probe tip. As a result, gases within the bubble were sampled between 3300–3700 ms. The 29-amu signal, possibly indicating formaldehyde, was the most abundant gas within the bubble, followed by N₂ and CO, H₂O, NO₂, and N₂O. Only a small amount of HCN was observed either above the boiling surface or within the bubble. NO was not observed above the pyrolyzing surface except for a small amount at 2500 ms and late in the formation of the bubble. It is interesting to note the very small amount of HCN and NO both in the bubble and above the surface under these conditions, because both of these species were observed in significant quantities for laser-assisted combustion.

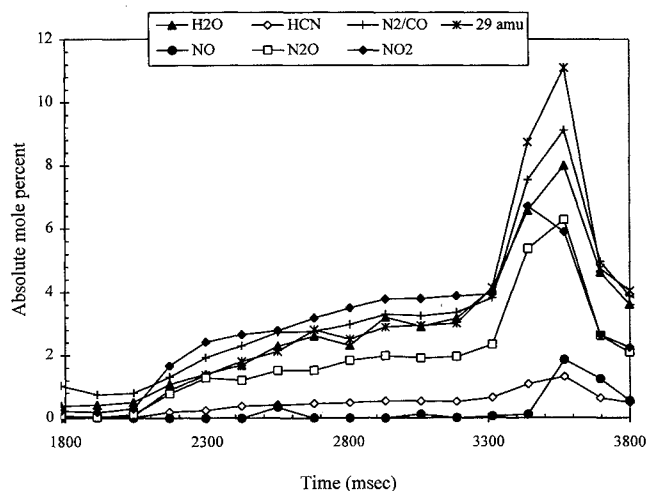


Fig. 2 Temporal variation of species for CO₂ laser-induced decomposition of RDX, including sampling within a bubble on the surface starting at 2500 ms.

Several species at significantly lower signal intensity were also detected including 42, 43, 70, 81, and 97 amu. The production of the species at 42 amu appeared to be driven by the external energy input. Both Schroeder² and Farber and Srivastava²⁰ list the structure of the species at 42 amu as CH₂NCH₂⁺, a radical that would not be detected by the MPMS system. However, Behrens and Bulusu^{3,4} found in their studies that the signal at 42 amu originated from 1-nitroso-3,5-dinitro-hexahydro-s-triazine (ONDNTA) at 206 amu and also observed the abundance of ONDNTA to rise gradually as the sample temperature increased between 195–215°C. It was likely that the melt-layer temperature for the test in Fig. 2 also rose gradually after the onset of gas evolution, during which time the abundance of the species, at 42 amu, was observed to increase until laser heating was terminated.

The species at 43 amu could be HNCO. This species has a stable structure (H—N=C=O) from a simple electron structure balance and should thus be detectable by the MPMS system. Interestingly, Behrens and Bulusu,^{3,4} Farber and Srivastava,²⁰ and Zhao et al.⁵ make no mention of this species, even as a fragment of other larger species. Goshgarian²¹ listed two structures for a species at 43 amu, but gave no profiles for this species. Korobeinichev et al.^{8,9} observed HNCO as a rapidly decaying profile near the surface. Oyumi and Brill⁶ have also observed HNCO in their thermolysis studies of RDX. Goshgarian²¹ observed lower molecular weight species to be dominant for his atmospheric pressures tests while higher molecular weight products became more important under high vacuum (10⁻⁷ torr). The studies of Behrens and Bulusu, Farber and Srivastava, and Zhao et al. were all conducted at pressures several orders of magnitude lower than the pressure of 0.5 atm employed by Oyumi and Brill, Korobeinichev et al., and the present study. Thus, the different pressures of the various studies may account for the presence or absence of 43 mol wt.

Behrens and Bulusu^{3,4} stated that the species they observed at 70 amu originated from the species at 97 amu. Two molecular structures for the species at 70 amu were given in the reviews by Boggs¹ and Schroeder.² Goshgarian²¹ observed the amount of a species at 70 amu to increase during melting for RDX, in agreement with the trends depicted in Fig. 2. The species at a molecular weight of 81 amu has also been observed by Zhao et al.⁵ and Goshgarian,²¹ who both proposed a structure for this molecule where the original ring structure for RDX remained intact, but all the NO₂ groups and three of the H atoms were removed from the ring structure. Fifer²² offered a scheme whereby the structure of this species was arrived at by successive elimination of three HONO molecules. Fifer then proposed that the 81-amu species may decompose to form three HCN molecules.

The only other studies identifying a species at 97 amu are those by Behrens and Bulusu^{3,4} and Snyder et al.,²³ which was referenced by Behrens and Bulusu. Behrens and Bulusu list three possible structures for this molecule and label it as oxy-s-triazine (OST). Farber and Srivastava²⁰ did not observe OST under conditions similar to those of Behrens and Bulusu. The fact that Zhao et al.⁵ did not observe OST in their infrared multiphoton dissociation (IRMPD) study of individual RDX molecules may imply that OST is produced by reactions within the heated bulk material.

In the present study, no species were observed with a molecular weight above 97 amu, even though the mass spectrometer was ramped up to 224 amu for the test at the lower eV and pressure setting. Behrens and Bulusu^{3,4} and Farber and Srivastava²⁰ have detected several species with molecular weights greater than 100 in slow heating rate tests, and Zhao et al.⁵ also detected species of this size in their IRMPD experiments. It is possible that the lack of observation of any species with molecular weights above 100 in the present study may be due to a difference in the decomposition mechanisms between the high heating rate and near atmospheric pressure

studies of the present work and the slow heating tests and very low pressures of these other studies.

Laser-Assisted Combustion

At 1 atm pressure and a heat flux of 400 W/cm^2 , the onset of the luminous flame was very abrupt, with the flame appearing almost instantaneously at roughly a steady-state height above the sample surface and remaining until the laser heating was removed. A thin violet flame zone separated from the surface by a nonluminous zone was observed. The flame ex-

hibited a slight dome shape due to both the nonuniformity of the laser beam profile and edge effects commonly observed for combustion of small propellant samples. At the condition of this test, the distance of the violet reaction zone from the surface was about 5 mm, although it did fluctuate approximately 1 mm during a test. At this heat flux, the surface layer did not exhibit the pronounced bubbling observed at the lower heat fluxes; the largest bubbles observed were less than $100 \mu\text{m}$ in diameter.

Figure 3 displays species profiles and element balances for this test. In this figure the zero distance position corresponds to the point where the sample probe contacted the surface in the video of the test; no corrections were made for a sampling offset. The species commonly reported for RDX decomposition were observed including NO_2 , NO , N_2O , HCN , H_2O , N_2 , CO , CO_2 , H_2 . A signal at 29 amu was also observed that could be due to H_2CO , and it was used to measure H_2CO in past studies by the authors.²⁴ However, recent work using the triple quadrupole mass spectrometer has shown that the signal at 29 amu contains at least one other species in addition to HCO .¹⁶ Also, Parr and Hanson-Parr¹⁰ have reported a maximum concentration of H_2CO of 0.005 under very similar experimental conditions. Thus, in the present results, the signal at 29 amu was not attributed to H_2CO , and was not included in the data.

Within approximately 0.5 mm of the sample surface, the most rapidly changing species are NO_2 , NO , and H_2O . Very little CO_2 is observed suggesting that the near surface temperature rise measured by Parr and Hanson-Parr¹⁰ is due to the production of water, not CO_2 . The high levels of CO_2 reported near the sample surface by Korobeinichev et al.^{8,9} may be due to the lower spatial resolution of that study compared to the present study. The results for NO and NO_2 near the surface show very similar shape and magnitudes to the results of Parr and Hanson-Parr, lending support for the modeling approach that combines their temperature profile with the species measurements of the present study. The species profiles for deflagration of RDX at 0.5 atm measured by Korobeinichev et al. indicate that N_2 and CO are of roughly the same concentration near the propellant surface. Thus, the present data are in reasonable agreement with these results.

Beyond 0.5 mm, NO and HCN are consumed, and CO , N_2 , and CO_2 all rise. N_2O , which remained relatively inert through the primary flame, is also consumed beyond 0.5 mm from the surface. The fluctuations in mole fractions, especially the rather large change at 4.5 mm, are a result of unsteadiness in the position of the final flame. The mole fractions between 4.5–5 mm represent species measured above the final flame and should be used to compare to the model results.

The bottom graph in Fig. 3 displays the element fractions for the species profiles. The element fractions in RDX are 0.286 for H, N, and O, and 0.143 for C. Variations near the sample surface may be due to diffusion effects or they may indicate that some species are not being detected. The unresolved species at 29 amu that has not been included in the data could have a significant impact on the near surface element balance.¹⁶ At larger distances, the high temperatures present in the flame may cause the room temperature calibration data to become inaccurate. The variations in the element balance means that the comparison to the model results must be made with care; precise agreement should not be expected.

Modeling of RDX Combustion

Using the measured mole fractions at the sample surface resulted in poor agreement between the model and the experimental data. The rate of consumption of NO_2 and production of NO were much too slow. In order to try to accelerate the NO_2 consumption, several variations in the initial species mole fractions were investigated. Initial mole fractions of H_2CO of 0.05, 0.10, and 0.15 were added to the measured

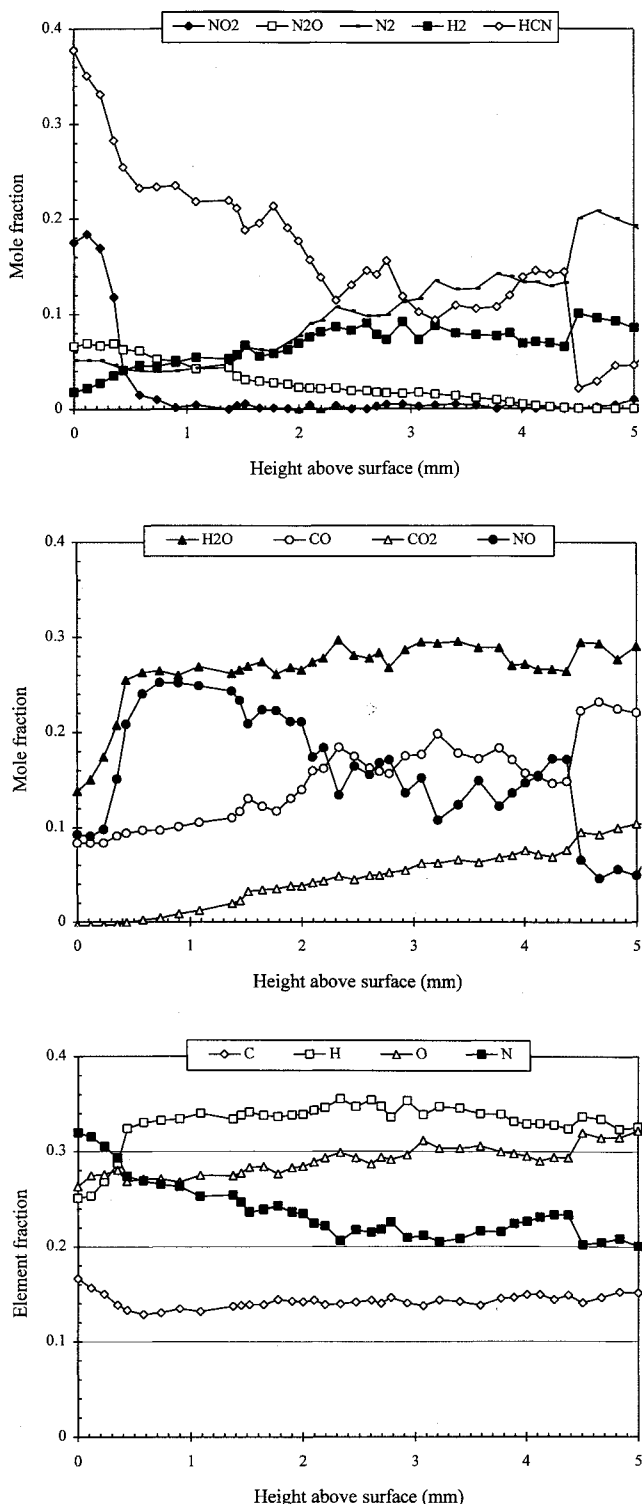


Fig. 3 Species profiles and element fractions above the surface of RDX during laser-assisted combustion at a heat flux of 400 W/cm^2 and a pressure of 1 atm.

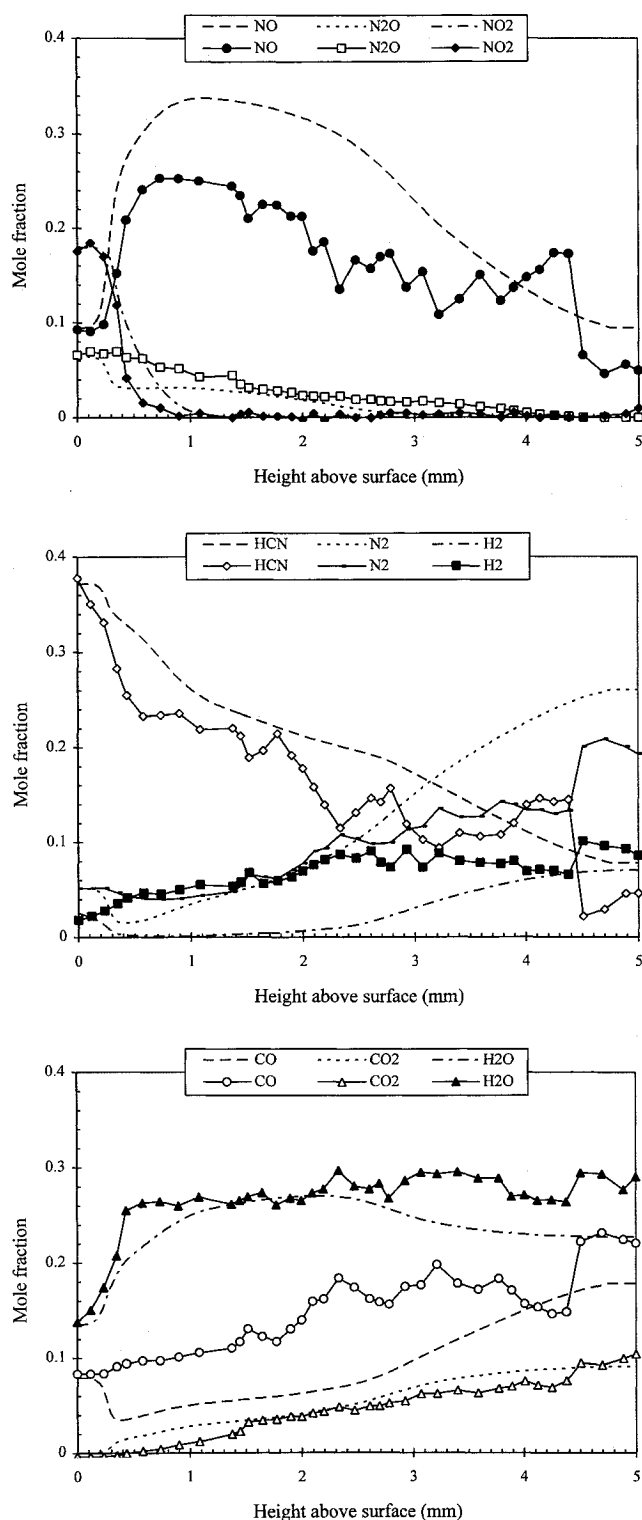


Fig. 4 Comparison of experimental data (lines with symbols) and model results (lines only) for initial conditions which include an RDX mole fraction of 0.50 at the sample surface.

species. This addition resulted in an increased consumption rate of NO_2 , but still did not consume it fast enough to match the data. A second change was to add RDX vapor into the initial species; this addition is physically reasonable because RDX vapor is known to exist at the surface. Because RDX vapor was not a measured quantity, a somewhat arbitrary choice of 0.50 mole fraction was made. To adjust for the addition of this RDX, the mole fractions of measured species were reduced to force the sum of the mole fractions to 1 at the sample surface.

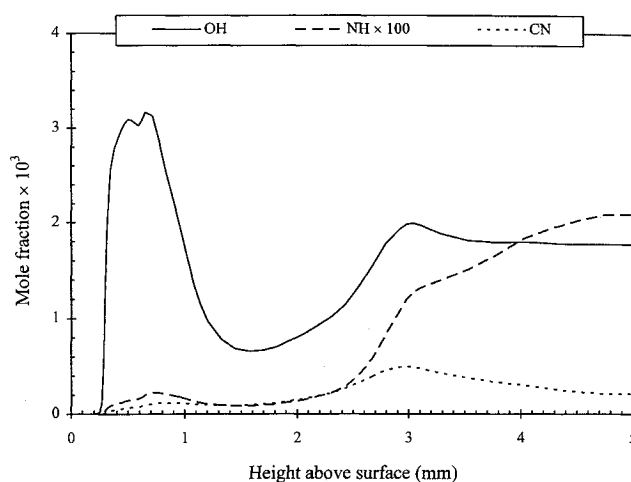


Fig. 5 Model predictions of the profiles of OH, NH, and CN.

Species profiles predicted by the model with the added RDX at the surface are presented in Fig. 4 along with the experimental results. To permit a direct comparison to the experimental data, only the predictions for measured species were used, and they normalized to give a mole fraction of 1 after the removal of RDX and all other species in the model that were not measured. In Fig. 4, the overall trends are in reasonable agreement with the measured results. However, the model does show unexpected decreases in N_2 , CO, and H_2 near the surface, as well as a rapid decrease in N_2O followed by a more gradual decrease, which is more in agreement with the experimental data. The rapid consumption of these species between 0.2–0.5 mm may be a result of the mole fraction of RDX that was chosen. The model results for NO show a gradual decrease consistent with the present data, but inconsistent with the results of Parr and Hanson-Parr,¹⁰ which show a very rapid decrease in NO mole fraction at approximately 2.5 mm from the sample surface.

Figure 5 presents the model predictions for three radical species measured by Parr and Hanson-Parr.¹⁰ The large OH peak near the surface is not reported in the data of Parr and Hanson-Parr, in this same region the CO_2 is much larger than the measured value. These two discrepancies could be due to the presence of too much H_2 at the surface, which is consumed and produces the large OH concentration. The OH then oxidizes CO to CO_2 more rapidly than occurs in the actual flame. Also, the NH and CN profiles do not show the rapid rise and fall observed by Parr and Hanson-Parr. Although the model shows reasonable trends for measured stable species, it does not reproduce the radical species data that is available. The reasons for the disagreement are not clear; they could be in the mechanism, in the experimental data, or in the modeling assumptions, in particular the one-dimensional assumption.

Summary

Both laser-induced decomposition and laser-assisted combustion of RDX were investigated in this study. During laser-induced decomposition, RDX displayed a liquid layer on the surface with considerable bubbling within the layer. The species detected above the surface included N_2 and CO at 28 amu, H_2O , NO_2 , N_2O , H_2 , and a species at 29 amu, perhaps formaldehyde, with only small amounts of HCN and NO. Minor species were also detected at molecular weights of 42, 43, 70, 81, and 97 amu, which have been reported by other researchers. The absence of higher molecular weight species in the present study may be due to the pressures used, as other studies reporting high molecular weight species were performed at very low pressure.

During laser-assisted combustion, a luminous flame appeared as a thin violet flame zone separated from the surface by a nonluminous region. Species profiles were measured that

gave evidence of a primary reaction zone involving the consumption of NO_2 . The reaction in the luminous flame zone consumes HCN, NO, and N_2O . Modeling of the results at 1 atm as a one-dimensional, premixed flame, using a mechanism of Yetter and Dryer,¹¹ produced reasonable agreement with the experimental profiles for stable species, but poor agreement for radical species indicating the need for further modeling and experimental studies.

Acknowledgments

This work was performed under the sponsorship of the Office of Naval Research, Mechanics Division, ONR Contract N00014-93-1-0080. The support and encouragement of R. S. Miller are greatly appreciated. Also the authors wish to acknowledge Tim Parr and Donna Hanson-Parr of the Naval Air Warfare Center for many discussions of the experimental and modeling results. Their comments and suggestions greatly enhanced the quality of this work.

References

- ¹Boggs, T. L., "Thermal Behavior of RDX and HMX," *Fundamentals of Solid-Propellant Combustion*, edited by K. K. Kuo and M. Summerfield, Vol. 90, Progress in Astronautics and Aeronautics, AIAA, New York, 1984, pp. 121–175, Chap. 3.
- ²Schroeder, M. A., "Critical Analysis of Nitramine Decomposition Data: Product Distributions from HMX and RDX Decomposition," Ballistic Research Lab., BRL-TR-2659, Aberdeen, MD, June 1985, pp. 1–117.
- ³Behrens, R., Jr., and Bulusu, S., "Thermal Decomposition of Energetic Materials. 4. Deuterium Isotope Effects and Isotopic Scrambling (H/D , $^{13}\text{C}/^{18}\text{O}$, $^{14}\text{N}/^{15}\text{N}$) in Condensed-Phase Decomposition of 1, 3, 5-Trinitrohexahydro-s-triazine," *Journal of Physical Chemistry*, Vol. 96, No. 22, 1992, pp. 8891–8897.
- ⁴Behrens, R., Jr., and Bulusu, S., "Thermal Decomposition of Energetic Materials. 3. Temporal Behaviors of the Rates of Formation of the Gaseous Pyrolysis Products from Condensed-Phase Decomposition of 1,3,5-Trinitro-hexahydro-s-triazine," *Journal of Physical Chemistry*, Vol. 96, No. 22, 1992, pp. 8877–8891.
- ⁵Zhao, X., Hints, E. J., and Lee, Y. T., "Infrared Multiphoton Dissociation of RDX in a Molecular Beam," *Journal of Chemical Physics*, Vol. 88, No. 2, 1988, pp. 801–810.
- ⁶Oyumi, Y., and Brill, T. B., "Thermal Decomposition of Energetic Materials 3. A High-Rate, In Situ, FTIR Study of the Thermolysis of RDX and HMX with Pressure and Heating Rate as Variables," *Combustion and Flame*, Vol. 62, 1985, pp. 213–224.
- ⁷Brill, T. B., Brush, P. J., Patil, D. G., and Chen, J. K., "Chemical Pathways at a Burning Surface," *Twenty-Fourth Symposium (International) on Combustion*, The Combustion Inst., Pittsburgh, PA, 1992, pp. 1907–1914.
- ⁸Korobeinichev, O. P., "Dynamic Probe Mass Spectrometry and Condensed-System Decomposition," *Combustion, Explosion, and Shock Waves*, Vol. 23, No. 5, 1987, pp. 565–576.
- ⁹Korobeinichev, O. P., Kuibida, L. V., and Paletskii, A. A., "A Study of Propellant Flame Structure by Mass-Spectrometric Sampling, Including MBMS," Conf. on Applications of Free-Jet, Molecular Beam Mass Spectrometric Sampling, Estes Park, CO, 1994.
- ¹⁰Hanson-Parr, D., and Parr, T., "RDX Flame Structure," *Proceedings of the 25th Symposium (International) on Combustion* (to be published).
- ¹¹Yetter, R. A., and Dryer, F. L., private communication, Princeton Univ., Princeton, NJ, 1993.
- ¹²Kee, R. J., Rupley, F. M., and Miller, J. A., "Chemkin-II: A Fortran Chemical Kinetics Package for the Analysis of Gas-Phase Chemical Kinetics," Sandia Rept. SAND89-8009, Albuquerque, NM, Sept. 1989.
- ¹³Kee, R. J., Rupley, F. M., and Miller, J. A., "The Chemkin Thermodynamic Data Base," Sandia Rept. SAND87-8215B, Albuquerque, NM, March 1990, reprinted Dec. 1990.
- ¹⁴Kee, R. J., Dixon-Lewis, G., Warnatz, J., Coltrin, M. E., and Miller, J. A., "A Fortran Computer Code Package for the Evaluation of Gas-Phase Multi-Component Transport Properties," Sandia Rept. SAND86-8246, Albuquerque, NM, Dec. 1986, reprinted Dec. 1990.
- ¹⁵Kee, R. J., Gricar, J. F., Smooke, M. D., and Miller, J. A., "A Fortran Program for Modeling Steady Laminar One-Dimensional Premixed Flames," Sandia Rept. SAND85-8240, Albuquerque, NM, Dec. 1985, reprinted Oct. 1990.
- ¹⁶Lee, Y., Tang, C.-J., and Litzinger, T. A., "A Study of the Gas-Phase Processes of RDX Combustion Using a Triple Quadrupole Mass Spectrometer," 31st JANNAF Combustion Meeting, Sunnyvale, CA, 1994.
- ¹⁷Bobeldijk, M., Van der Zande, W. J., and Kistemaker, P. G., "Simple Models for the Calculation of Photoionization and Electron Impact Ionization Cross-Sections of Polyatomic Molecules," *Chemical Physics*, Vol. 179, No. 2, 1994, pp. 125–130.
- ¹⁸Melius, C. F., "The Gas-Phase Flame Chemistry of Nitramine Combustion," 25th JANNAF Combustion Meeting, CPIA Publ. 498, Vol. II, Oct. 1988, pp. 155–162.
- ¹⁹Ermolin, N. E., Korobeinichev, O. P., Kuibida, L. V., and Fomin, V. M., "Processes in Hexogene Flames," *Combustion, Explosion, and Shock Waves*, Vol. 24, No. 4, 1988, pp. 400–409.
- ²⁰Farber, M., and Srivastava, R. D., "Mass Spectrometric Investigation of the Thermal Decomposition of RDX," *Chemical Physics Letters*, Vol. 64, No. 2, 1979, pp. 307–310.
- ²¹Goshgarian, B. B., "The Thermal Decomposition of Cyclotrimethylene-trinitramine (RDX) and Cyclotetramethylene-tetranitramine (HMX)," Air Force Rocket Propulsion Lab., AFRPL-TR-78-76, Oct. 1978.
- ²²Fifer, R. A., "Chemistry of Nitrate Ester and Nitramine Propellants," *Fundamentals of Solid-Propellant Combustion*, edited by K. K. Kuo and M. Summerfield, Vol. 90, Progress in Astronautics and Aeronautics, AIAA, New York, 1984, pp. 177–237, Chap. 4.
- ²³Snyder, A. P., Kremer, J. H., Liebman, S. A., Schroeder, M. A., and Fifer, R. A., "Characterization of Cyclotrimethylenetrinitramine (RDX) by N,H Isotope Analyses with Pyrolysis-Atmospheric Pressure Ionization Tandem Mass Spectrometry," *Organic Mass Spectrometry*, Vol. 24, No. 1, 1989, pp. 15–21.
- ²⁴Fetherolf, B. L., and Litzinger, T. A., "Chemical Structure of the Gas Phase Above Deflagrating RDX: Comparison of Experimental Measurements and Model Predictions," 30th JANNAF Combustion Meeting, Monterey, CA, Nov. 1993.